Physica B 407 (2012) 1634–1637

Contents lists available at SciVerse ScienceDirect

Physica B

journal homepage: www.elsevier.com/locate/physb

Pt–Al_2O_3 nanocoatings for high temperature concentrated solar thermal power applications

Zebib.Y. Nuru [a,b,c,*], C.J. Arendse [b], R. Nemutudi [a], O. Nemraoui [a], M. Maaza [a,b,c]

[a] NANOAFNET, MRD- iThemba LABS, National Research Foundation,1 Old Faure road, Somerset West, South Africa
[b] Department of Physics, University of Western Cape, Private Bag X 17, Belleville, South Africa
[c] African Laser Centre, CSIR campus, P.O. Box 395, Pretoria, South Africa

ARTICLE INFO

Available online 25 September 2011

Keywords:
Solar thermal absorbers
Metal–dielectric composites
Multilayer coating
Selective absorber
Platinum
Alumina
Absorbance

ABSTRACT

Nano-phased structures based on metal–dielectric composites, also called cermets (ceramic–metal), are considered among the most effective spectral selective solar absorbers. For high temperature applications (stable up to 650 °C) noble metal nanoparticles and refractory oxide host matrices are ideal as per their high temperature chemical inertness and stability: Pt/Al_2O_3 cermet nano-composites are a representative family. This contribution reports on the optical properties of Pt/Al_2O_3 cermet nano-composites deposited in a multilayered tandem structure. The radio-frequency sputtering optimized Pt/Al_2O_3 solar absorbers consist of stainless steel substrate/ Mo coating layer/ Pt–Al_2O_3/ protective Al_2O_3 layer and stainless steel substrate/ Mo coating layer /Pt–Al_2O_3 for different composition and thickness of the Pt–Al_2O_3 cermet coatings. The microstructure, morphology, theoretical modeling and optical properties of the coatings were analyzed by the x-ray diffraction, atomic force, microscopy, effective medium approximation and UV–vis specular and diffuse reflectance.

1. Introduction

Utilization of thermal energy obtained from solar radiation using solar collectors requires efficient spectrally selective solar absorber surfaces. There are several design options and physical mechanisms creating such selectively solar absorbing surfaces. Selective absorber surface coatings can be classified into six distinct types: (i) intrinsic, (ii) semiconductor–metal tandems, (iii) multilayered absorbers, (iv) selectively solar-transmitting coatings on a blackbody-like absorber, (v) textured surfaces and (vi) metal–dielectric composite coatings. Intrinsic absorbers use a material possessing intrinsic properties that result in the desired spectral selectivity. Semiconductor–metal tandems absorb short wavelength radiation because of the semiconductor band gap and have low thermal emittance as a result of the metal layer. Multilayered absorbers use multiple reflections between layers to absorb light and can be tailored to be efficient selective absorbers. Textured surfaces can produce high solar absorptance by multiple reflections among them one could quote needle-like, dendritic, or porous microstructures. Additionally, selectively solar-transmitting coatings on a blackbody-like absorber are also used but are typically used in low-temperature applications. Metal–dielectric composites, a case reported in this contribution, consist of nano-scaled metal particles in a dielectric or ceramic host matrix. This latter class of so called cermet "ceramic–metal" type solar absorbers exhibit high absorption and high reflection in the UV–vis and NIR, respectively, over large solar spectrum range. In addition, when such a composite cermet-coating is formed on a highly reflecting metal surface, the resulting tandem coating has a good spectral selectivity [1–7]. The optimum characteristics of spectrally selective surface for high temperature must have both high solar absorptance α and low thermal emittance ε above 400 °C. This behavior can be achieved using multilayered structures: A non oxidizing metallic layer with a maximum reflection in the infrared region "onto the substrate or acting as substrate itself", the highly absorbing cermet layer and anti-reflection layer to suppress front surface reflection. Currently, coatings like Mo–Al_2O_3, Ni–Al_2O_3,Fe–Al_2O_3 and Co–Al_2O_3 do not have the required thermal stability at high temperature for solar thermal power plant applications [1–3]. However, co-evaporated graded Pt–Al_2O_3 cermet coating on Pt coated glass with an antireflection layer appeared to be stable up to 600 °C in air [4,8–11]. Moreover graded, uniform and Al_2O_3/Pt–Al_2O_3/Al_2O_3 type onto Pt base layer confirmed the durability of graded Pt–Al_2O_3 cermet as reported by Bunshah et al. [5]. The optical properties of such composites are obtained from effective dielectric permeability of the composite, which can be related to the constituents in the effective medium or renormalization theories. These theories and specifically the effective medium theory can be used to estimate the

* Corresponding author at. NANOAFNET, MRD- iThemba LABS, National Research Foundation,1 Old Faure road, Somerset West, South Africa.
Tel.: +27 734935948(mob); fax: +27 0865889927, +27 21 8433543.
E-mail address: Zebib@tlabs.ac.za (Zebib.Y. Nuru).

0921-4526/$ - see front matter © 2011 Elsevier B.V. All rights reserved.
doi:10.1016/j.physb.2011.09.104

optical performance of the cermet. We report on the optimization and further selectivity improvement of radio-frequency sputtered graded Pt–Al_2O_3 deposited on Mo base layer exhibiting a high solar absorption and a significant thermal stability up to 650 °C in air with and without antireflection layers.

2. Experimental results and discussion

As a target for the radio-frequency synthesis of the above mentioned Pt–Al_2O_3 cermet coatings, an Al_2O_3 disk "13 cm in ∅" with circular small Pt pellets "∼5 mm in ∅" placed on it were used. The Pt pellets were placed in a hexagonal array on the Al_2O_3 disk target to ensure an isotropic deposition of Pt and Al_2O_3. The composition of the films was varied according to the number of Pt pellets used. The optimized working pressure was fixed to $\sim 10^{-2}$ Torr without heating the samples' stainless steel substrates as was substantiated by early studies on pure Pt–Al_2O_3 samples [8–12]. In this experimental part, the focus has been on the optimized multilayered cermet samples with and without reflecting layers; they are as follows: Pt–Al_2O_3/Mo/Stainless steel substrate, anti-reflecting layer of Al_2O_3/Pt–Al_2O_3/Mo/Stainless steel substrate.

The optimized Pt concentration in the Pt–Al_2O_3 cermet layer i.e. in terms of the Pt filling factor "f value", was deduced by modeling using the Brugemann effective medium approximation. The Pt–Al_2O_3 cermet layer is treated as an isotropic inhomogeneous medium with a random mixture of metallic Pt nano-particles in the host dielectric matrix with a filling factor f and dielectric constants ε_m "Pt" and ε_d "Al_2O_3" as homogeneous medium with an effective dielectric constant ε_{eff} given by $[f(\varepsilon_m-\varepsilon_{eff})/(\varepsilon_m+2\ \varepsilon_{eff})+(1-f)\ (\varepsilon_d-\varepsilon_{eff})/(\varepsilon_d+2\varepsilon_{eff})]$. Using the tabulated values of ε_{Pt} and ε_{Al2O3} from the standard Palik's database, the preliminary modeling calculations allowed the determination of the value of the Pt filling factor "f" at about ∼0.34. As reported in Fig. 1, the simulations allowed, in addition, to demonstrate that thin films of Pt–Al_2O_3 onto Mo buffer IR reflective layer/stainless steel substrates have better solar optical absorption characteristics than thick Pt–Al_2O_3 cermet ones. The optimized Pt–Al_2O_3 thin film thickness was found to be about ∼70 nm with a Mo buffer layer of ∼150 nm onto the considered stainless steel substrates. Such a cermet coating /Mo/stainless steel substrate exhibits average theoretical reflectivities $\leq 10\%$ and $\geq 70\%$ in the UV–vis-NIR and FIR spectral ranges of 200–1200 nm and above 1200 nm, respectively. The thick Pt–Al_2O_3 cermet coating/Mo/stainless steel has a constant low reflectivity of about 20% all over the UV–vis-NIR and FIR range.

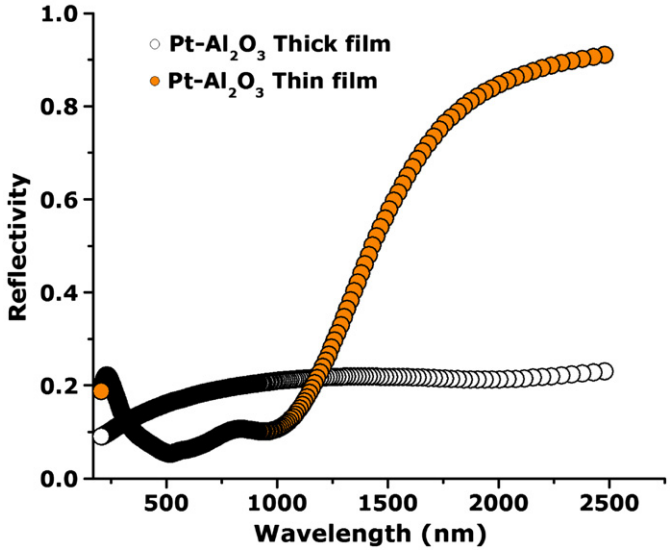

Fig. 1. Theoretical reflectivity profiles of thin "∼70 nm" and thick "∼1 μm" Pt–Al_2O_3 cermet coatings onto stainless steel substrates. The Pt filling factor in the Pt–Al_2O_3 cermet coatings is ∼0.34.

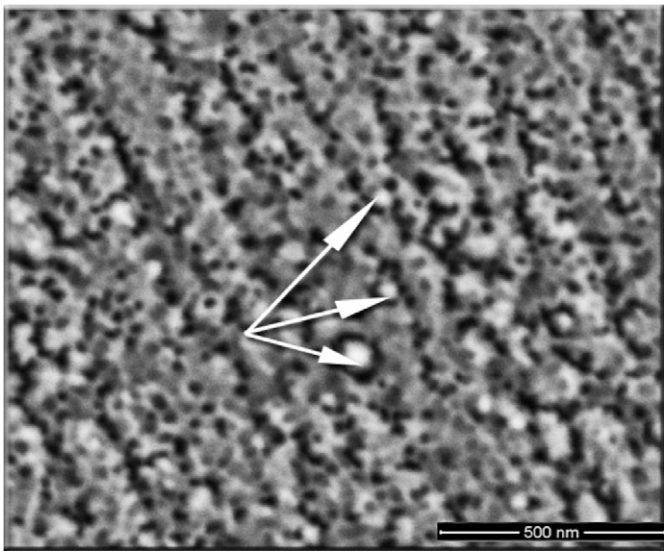

Fig. 2. Scanning electron microscopy of the optimized cermet sample: anti-reflecting layer of Pt/∼70 nm Pt–Al_2O_3/∼150 nm Mo/∼0.5 mm Stainless steel substrate.

Following this modeling phase, the optimized synthesized cermet samples were characterized from morphological, crystallographic and optical view points using scanning electron microscopy "SEM", atomic force microscopy "AFM", X-rays diffraction "XRD" and diffuse reflection scattering "specular and non-specular modes". Fig. 2 reports a typical SEM surface morphology of Pt–Al_2O_3 thin film/Mo buffer layer/stainless steel substrate with f ∼0.34. The corresponding cermet film exhibits a tortuous surface morphology with Pt nano-particles distributed isotropically in the basal plane. Their average diameter and inter-particles distance are statistically about 4–6 nm and 7–10 nm, respectively. Fig. 3 depicts a representative AFM surface scanning of such a sample. More specifically, the cermet sample's surface exhibits two type of surface topographies; highly disordered and semi-ordered stripes type zones. These latter regions of semi-disordered "stripes" have an average length of ∼0.41 μm consisting of 1-D chains-like of a length of about ∼0.41 μm. These 1-D chains-like are spatially ordered and consist of crystallites with an average diameter of about 250 nm. The crystallites, in the disordered regions have approximately an identical average size. The average roughness value is of about 8.8 nm. Relatively speaking, this roughness value is comparable to the average diameter and inter-particles distance, which were found to be about 4–6 nm and 7–10 nm, respectively. Hence, once could deduce that the surface topography is controlled by the Pt nano-particles. The nature of the ordered regions cannot be explained for the moment; it will be investigated methodically to shed-light its origin. Fig. 4 reports the crystallographic orientations of the optimized Al_2O_3/Pt–Al_2O_3/Mo/Stainless steel and the Pt–Al_2O_3/Mo layer/Stainless steel samples. Taking into account the absorption coefficients of Pt, Mo and Alumina [9–12] while considering the fact that the anti-reflecting layer of Al_2O_3, cermet layer of Pt–Al_2O_3 as well as the buffer IR reflective metallic layer of Mo are thin, the probing X-rays impinging the samples do penetrate and reach the stainless steel substrate. Indeed as sustained by Fig. 4, while the stainless steel substrate is highly crystalline with a net (1 1 1), (2 0 0) and (2 2 0) texturing, the buffer IR reflecting